Supporting Information

Schober and Fuchs 10.1073/pnas.1107807108

SI Methods

Mice. $T\beta RII^{flox}$ (1), FAK^{flox} (2), and *K14-Cre* (3) mice have been described. Single conditional KO mice were generated by mating *K14-Cre* mice to $T\beta RII^{flox}$ mice (4). Progeny mice were bred to FAK^{flox} mice and backcrossed to either $T\beta RII^{flox}$ mice to generate stud males that carry *K14-Cre*; $T\beta RII^{flox/flox}$; $FAK^{flox/+}$ alleles or to FAK^{flox} mice to generate stud males that carry *K14-Cre*; $T\beta RII^{flox/+}$; $FAK^{flox/flox}$ alleles. *K14-Cre*; $T\beta RII^{flox/flox}$; $FAK^{flox/+}$ stud males were mated to $T\beta RII^{flox/flox}$; $FAK^{flox/+}$ female mice, and *K14-Cre*; $T\beta RII^{flox/+}$; $FAK^{flox/flox}$ stud males were mated to $T\beta RII^{flox/+}$; $FAK^{flox/flox}$ female mice. All experiments were performed on littermate mice which were obtained from the same breeding; mice that did not carry the *K14-Cre* allele were used as wild-type controls. Mouse genotypes were determined by PCR. The genetic background of these mice is mostly C57Bl6.

Complete Carcinogenesis. Complete carcinogenesis was performed as described (4, 5). Mice were treated twice a week, starting at 7 wk of age, for up to 25 wk with 5 μg of 7,12-dimethylbenz[α]anthracene (DMBA) (D3254-1G; Sigma) dissolved in acetone. Mice were monitored weekly to assess tumor numbers, size, and appearance. This protocol generates squamous cell carcinomas (SCCs) with high frequency in contrast to single-dose DMBA followed by repetitive tumor-promoting agent (TPA) treatments.

Hair Follicle Bulge and Epidermal Progenitor Cell Preparation. Hair follicle (HF) stem cells (SCs) and basal epidermal progenitors were isolated from 8-wk-old female C57Bl6 mice where HFs were in the telogen (resting) stage of the hair cycle as previously described (6, 7). Briefly, back skin was incubated in 0.25% trypsin (Gibco) at 37 °C for 1 h. Epidermis and hair follicles were scraped off the subcutaneous fat and lower dermis with a dull scalpel and were passed through a 40-μm cell strainer. The single-cell suspension was washed with PBS containing 2% chelexed FBS and was incubated with surface antibodies for FACS.

Primary Keratinocyte Culture and Colony Formation Assays. Epidermis was separated from newborn mouse skin by enzymatic treatment with dispase, and single-cell suspensions of primary epidermal keratinocytes then were generated by trypsin treatment. Isolated cells were plated on 3T3 feeder layers and cultured as previously described (7, 8). Colony formation assays were performed by plating 10^4 cells per well on confluent 3T3 feeder layers in six-well plates. Colony numbers were counted 10 d after plating. Cells were fixed in 4% formaldehyde and stained with 1% Rhodamine B in PBS.

Flow Cytometry. Epidermal progenitor cells and HF bulge SCs were isolated based on staining for CD49f- phycoerythrin (PE) (cloneGoH3; 555736; BD Pharmingen) and $CD34^-$ Alexa Fluor 647 (clone RAM34; 51–0341; eBioscience) (6, 7). Primary SCC cells were isolated based on staining for CD49f-FITC (clone GoH3; 555735; BD Pharmingen), CD29-Pacific Blue (clone HMβ1–1; 102223; BioLegend), CD34-Alexa Fluor 647 (clone RAM34; 51–0341; eBioscience), CD11b-biotin (clone M1/70; BAM1124; R&D Systems), CD31-biotin (13–0311; eBioscience), CD45-biotin (clone OX-1; 554876; BD Pharmingen), and streptavidin-PE (554061; BD Pharmingen). Dead cells were excluded based on negative propidium iodide staining (0.5 μg/mL). Detector voltage was defined and compensation matrix was determined using antibody-labeled microbeads to ensure reproducibility between experiments. Secondary cancer stem cells (CSCs) were isolated based on live/dead exclusion by DAPI (0.6 μg/mL), RFP, and staining for CD29-Alexa Fluor 700 (clone HMβ1–1; 102218; BioLegend), CD49f-PerCP-Cy5.5 (clone GoH3; 313618; BioLegend), and CD34-Alexa Fluor 647 (clone RAM34; 51–0341) (eBioscience). Compensation matrix was determined by single-color–stained Nude back skin epidermis. RFP compensation settings were determined using an unstained SCC cell suspension. FACS sorts were performed on a FACS Aria2 (BD Biosciences) with a two-way collection to the right and left of the stream to ensure the highest purity. Sort quality and potential contamination were determined in postsort experiments. FACS analyses were performed on a BD LSRII analyzer (BD Biosciences) using FACSDiva software. FACS data were postprocessed and analyzed using FlowJo 7.6 software.

RNA Isolation and Microarray Analyses. Total RNAs were isolated from cells sorted directly into TRIzol LS (Invitrogen). RNA quality was assessed on an Agilent 2100 Bioanalyzer. Two rounds of amplification/labeling of 200 ng RNA were performed to obtain biotinylated cRNAs for hybridization onto Affymetrix GeneChip Mouse Genome MOE430 2.0 oligonucleotide microarrays at the Genomics Core Laboratory of Memorial Sloan-Kettering Cancer Center (New York). Two independent samples per respective genotype were used for data analyses. Scanned microarray images were imported into Gene Pattern (Broad Institute) (9, 10) and preprocessed using ExpressionFileCreator to generate signal values and present/absent calls for each probe using the Robust Multichip Average statistical expression algorithm with background subtraction. Hierarchical clustering was performed on preprocessed data sets using a pairwise complete-linkage clustering method in combination with Pearson correlation as a column distance measure and uncentered correlation as a row distance measure (11). Data were visualized using Gene Pattern's HierarchicalClusteringViewer. Differential gene-expression analysis was performed on preprocessed data sets using Gene Pattern's ComparativeMarkerSelection module using default settings. All possible permutations were performed. Differentially expressed gene sets were filtered using Gene Pattern's ComparativeMarkerSelectionViewer module based on a fold change >2, and a false-discovery rate (FDR) <0.05. Derived data sets were visualized in Gene Pattern's HeatMapViewer. To derive differentially expressed gene sets from $CD34^{hi}$ CSCs, $CD34^{hi}$ expression values first were divided by the corresponding $CD34^{lo}$ expression values of preprocessed data sets for additional normalization. Differential expression values then were compared and filtered as described above using Gene Pattern's DifferentialGeneExpression and ComparativeMarkerSelectionViewer modules. The Venn diagram illustrating the core SCC signature genes was generated in Gene Pattern based on genes that were differentially upregulated by more than twofold in SCC compared with either epidermal progenitor cells or bulge SCs. Genes derived from Differential Gene Expression analyses were classified using the functional annotation tool from DAVID Bioinformatics Resources 6.7 (12, 13).

Retroviral Infection. Retrovirus was produced in Phoenix EcoPack cells (National Gene Vector Biorepository) after transfection of a pBABE-PGK-luc-mrfp1-tk triple-modality reporter. pBABE-PGK-luc-mrfp1-tk was generated from a cmv–luc-mrfp1-tk reporter construct (14).

Histology and Immunofluorescence. Tissues were embedded in Optimum Cutting Temperature compound, and frozen sections were fixed in 4% paraformaldehyde and subjected to immunofluorescence microscopy or H&E staining and histological analyses. The following antibodies were used in immunofluorescence staining in this study: keratin 5 (K5) (guinea pig; 1:300; E.F.); loricrin [rabbit (Rb); 1:2,000, E.F.]; involucrin (Rb; 1:2,000; Covance); keratin 8 [rat (Rt); 1:1,000; DSHB TROMA-I]; keratin 18 (Rb; 1:1,000; E.F.); Sex-determining region Y (SRY)-box 9 (Sox9) (Rb; 1:1,000, E.F.); Sox2 (Rb; 1:1,000; ab5603; Abcam); CD44-APC (allophycocyanin) (Rt; 1:500; 559250; BD); CD34-biotinylated (Rt; 1:100; BD); CD29 (Rt; 1:1,000; Chemicon); CD104 (Rt; 1:1,000; BD); and keratin 6 (Rb; 1:300; E.F.). Images were acquired using Metamorph 7.5 software on a Zeiss Axioplan2 upright microscope equipped with a Zeiss Plan Apochromat 20×, NA0.8 objective, a 0.63× projection lens, and a Hammamatsu OrcaER digital camera. Automated image analysis was performed using Metamorph software and its multiwavelength cell-scoring application. Confocal images were acquired on a Zeiss 510-Meta scanning confocal microscope.

Western Blotting. Western blotting was performed using 4–12% NuPAGE Bis-Tris gradient gels (Invitrogen) and an Odyssey LiCor infrared scanner as previously described (15). Primary antibodies were NFATc1 (mouse; 1:2,000; ab2794; Abcam), α-tubulin (mouse; 1:4,000; DM1A; Sigma), Sox9 (Rb; 1:4,000; E.F.), and K6 (Rb; 1:4,000; E.F.).

1. Levéen P, et al. (2002) Induced disruption of the transforming growth factor beta type II receptor gene in mice causes a lethal inflammatory disorder that is transplantable. *Blood* 100:560–568.
2. Beggs HE, et al. (2003) FAK deficiency in cells contributing to the basal lamina results in cortical abnormalities resembling congenital muscular dystrophies. *Neuron* 40:501–514.
3. Vasioukhin V, Degenstein L, Wise B, Fuchs E (1999) The magical touch: Genome targeting in epidermal stem cells induced by tamoxifen application to mouse skin. *Proc Natl Acad Sci USA* 96:8551–8556.
4. Guasch G, et al. (2007) Loss of TGFbeta signaling destabilizes homeostasis and promotes squamous cell carcinomas in stratified epithelia. *Cancer Cell* 12:313–327.
5. Hennings H, et al. (1993) FVB/N mice: An inbred strain sensitive to the chemical induction of squamous cell carcinomas in the skin. *Carcinogenesis* 14:2353–2358.
6. Blanpain C, Lowry WE, Geoghegan A, Polak L, Fuchs E (2004) Self-renewal, multipotency, and the existence of two cell populations within an epithelial stem cell niche. *Cell* 118:635–648.
7. Nowak JA, Fuchs E (2009) Isolation and culture of epithelial stem cells. *Methods Mol Biol* 482:215–232.
8. Rheinwald JG, Green H (1975) Serial cultivation of strains of human epidermal keratinocytes: The formation of keratinizing colonies from single cells. *Cell* 6:331–343.
9. Kuehn H, Liberzon A, Reich M, Mesirov JP (2008) Using GenePattern for gene expression analysis. *Curr Protoc Bioinformatics* Chapter 7:Unit 7 12.
10. Reich M, et al. (2006) GenePattern 2.0. *Nat Genet* 38:500–501.
11. Eisen MB, Spellman PT, Brown PO, Botstein D (1998) Cluster analysis and display of genome-wide expression patterns. *Proc Natl Acad Sci USA* 95:14863–14868.
12. Dennis G, Jr., et al. (2003) DAVID: Database for annotation, visualization, and integrated discovery. *Genome Biol* 4:3.
13. Huang W, Sherman BT, Lempicki RA (2009) Systematic and integrative analysis of large gene lists using DAVID bioinformatics resources. *Nat Protoc* 4:44–57.
14. Ray P, Tsien R, Gambhir SS (2007) Construction and validation of improved triple fusion reporter gene vectors for molecular imaging of living subjects. *Cancer Res* 67: 3085–3093.
15. Williams SE, Beronja S, Pasolli HA, Fuchs E (2011) Asymmetric cell divisions promote Notch-dependent epidermal differentiation. *Nature* 470:353–358.

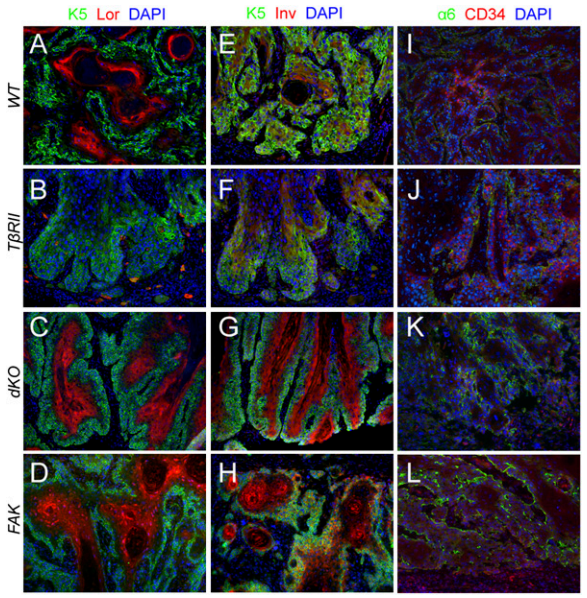

Fig. S1. TGF-β receptor-II (TβRII)/TGF-β and focal adhesion kinase (FAK)/integrin signaling markedly influence SCC composition. (*A–H*) Epidermal differentiation markers loricrin (Lor) (*A–D*) and involucrin (Inv) (*E–H*) show reduced expression in $T\beta RII^{KO}$ (*B* and *F*) compared with *dKO* (*C* and *G*) and FAK^{KO} (*D* and *H*) SCCs. K5 marks undifferentiated cells at the tumor–stroma interface. (*I–L*) The CSC marker CD34 is expanded in $T\beta RII^{KO}$ (*J*) compared with *dKO* (*K*) and FAK^{KO} (*L*) SCCs. α6 integrin demarcates the tumor–stroma interface.

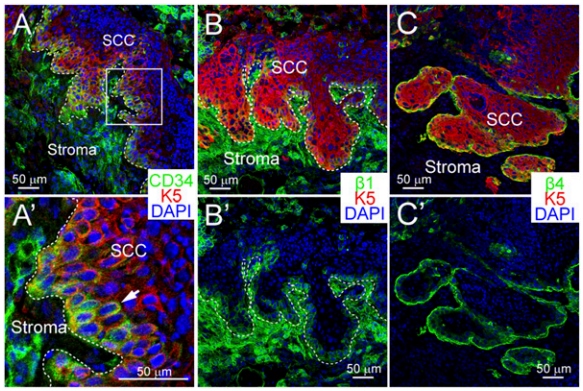

Fig. S2. Integrins and CD34 are expressed at the tumor–stroma interface of cutaneous SCCs. (*A* and *A′*) In SCCs, K5 is expressed in the undifferentiated cells at the tumor–stroma interface. Some K5$^+$ cells express CD34. Although many CD34$^+$ cells are in direct contact with the stroma, CD34$^+$ cells also can be found at a distance from the tumor–stroma interface. β1 integrin (*B* and *B′*) and β4 integrin (*C* and *C′*) are highly expressed in K5$^+$ cells at the tumor–stroma interface and also in some clusters of suprabasal cells. β1 integrin also is expressed in a large number of stromal cells, which are distinguished from epithelial cells by their lack of α6 integrin expression.

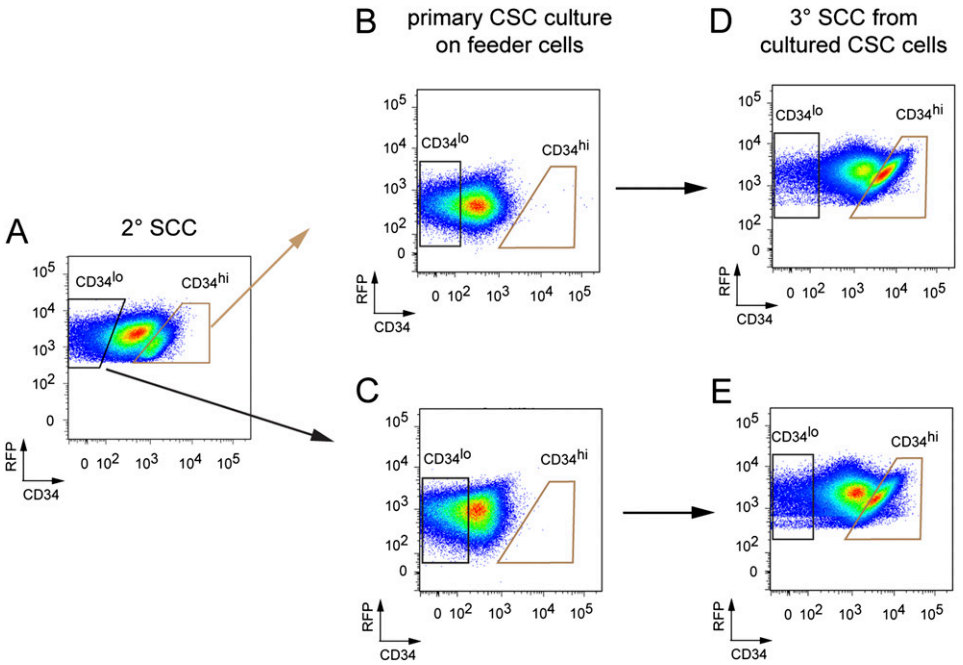

Fig. S3. CD34 expression depends on tumor microenvironment. (*A*) CD34^{hi}α6^{hi}β1^{hi} and CD34^{lo}α6^{hi}β1^{hi} CSC populations are separated by FACS. Culture of CD34^{hi}α6^{hi}β1^{hi} CSCs (*B*) and CD34^{lo}α6^{hi}β1^{hi} CSCs (*C*) on 3T3 feeder layers does not sustain high CD34 expression. (*D* and *E*) Transplantation of these cultures onto *Nude* recipient mice reestablishes CD34^{hi}α6^{hi}β1^{hi} and CD34^{lo}α6^{hi}β1^{hi} CSC populations.

Dataset S1. CSC signature genes

Dataset S1 (XLS)

Affymetrix probe sets and their annotated genes for mRNAs up-regulated more than twofold with an FDR <0.05 in FACS-purified CSC populations in comparison with mRNAs from epidermal progenitor cells (Epi) and HF-SCs purified with the same surface markers. Each column represents the average of two data sets for CSCs obtained from independent SCCs of the indicated genotype. Gene names are listed in alphabetical order.

Dataset S2. Genes that are differentially expressed in CSCs and HF-SCs

Dataset S2 (XLS)

Affymetrix probe sets and their annotated genes for mRNAs up-regulated or down-regulated more than twofold with an FDR <0.05 in FACS-purified CSC populations in comparison with HF-SCs. Each column represents the average of two data sets obtained from independent SCCs of the indicated genotype. Genes are sorted based on a significance score. The top 200 genes that were up-regulated preferentially in CSCs are shown at the top of the table. Below the horizontal red line are listed the top 200 genes that were preferentially down-regulated in CSCs (up-regulated in HF-SCs).

Dataset S3. Genes that are differentially expressed in CSCs and epidermal progenitor cells

Dataset S3 (XLS)

Affymetrix probe sets and their annotated genes encoding mRNAs that were up-regulated more than twofold with an FDR <0.05 in FACS-purified CSC populations in comparison with mRNAs from epidermal progenitor cells (Epi) purified using the same surface markers. Each column represents the average of two data sets obtained from CSCs of independent SCCs of the indicated genotype. Genes are sorted based on a significance score. Genes up-regulated in CSCs are shown at the top of the table. Below the horizontal red line are listed the top 200 genes that were preferentially down-regulated in CSCs (up-regulated in Epi).

Dataset S4. Genes that are differentially expressed in fast- and slow-cycling CSCs

Dataset S4 (XLS)

Affymetrix probe sets and their annotated genes up-regulated more twofold in fast- or slow-cycling $CD34^{hi}\alpha6\beta1^{hi}$ CSCs, respectively. Fast-cycling $CD34^{hi}\alpha6\beta1^{hi}$ CSCs were obtained from $T\beta RII^{KO}$ SCCs; slow-cycling $CD34^{hi}\alpha6\beta1^{hi}$ CSCs were obtained from *dKO* and FAK^{KO} SCCs. Differential expression values in $CD34^{hi}\alpha6\beta1^{hi}$ and $CD34^{lo}\alpha6\beta1^{hi}$ CSCs were determined for each individual SCC and where shown are provided as a $\log_2$ ratio. Genes then were sorted based on a significance score. Genes preferentially up-regulated in fast-cycling $CD34^{hi}\alpha6\beta1^{hi}$ CSCs are shown at the top of the table. Genes preferentially up-regulated in slow-cycling $CD34^{hi}\alpha6\beta1^{hi}$ CSCs are shown below the horizontal red line. Note that, overall, CSCs from each of these populations were more similar to each other than to normal skin stem cell populations. However, these comparisons show that slow-cycling CSCs preferentially show higher levels of extracellular matrix and adhesion gene expression, and faster-cycling CSCs preferentially show elevated levels of cell-cycle gene expression.